Applied Mathematical Biosystems, Volume 2, Issue 1, (Jan-Jun 2026), 13-25

Applied Mathematical Biosystems

journal homepage: https://ambjournal.com

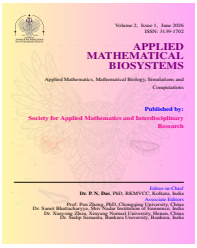

Mathematical Modeling of Serial Killer Dynamics and its Prevention Using Machine Learning Based Physics Informed Neural Networks

Tshering Dorjee Bhutia[1], Biswadip Pal[2], Purnendu Sardar[3], Santosh Biswas[3] and Krishna Pada Das[4]

[1]*Department of Mathematics, Ramakrishna Mission Residential College (Autonomous), Narendrapur, Kolkata, India*
[2]*Department of Computer Science, Ramakrishna Mission Residential College (Autonomous), Narendrapur, Kolkata, India*
[3]*Centre for Mathematical Biology and Ecology, Department of Mathematics, Jadavpur University, 188, Raja S.C. Mallick Road, Kolkata - 700032, India*
[4]*Department of Mathematics, Mahadevananda Mahavidyalaya, Barrackpore, Kolkata - 700120, West Bengal, India*

Abstract

Serial killer activity is a complex social threat that traditional criminology often struggles to predict quantitatively. To better understand this phenomenon, we propose a mathematical modeling framework inspired by epidemiology. The population is divided into four compartments: at-risk individuals (A), active serial killers (S), prevention programs (P), and law enforcement (L). Their interactions are described by a system of nonlinear differential equations representing the spread and control of criminal behavior. We first establish fundamental analytical properties of the model, including positivity and boundedness of solutions. Two equilibrium states are identified: a crime-free equilibrium and a persistent (Persistent Crime) crime state. A threshold parameter, the basic reproduction number R_0, determines stability; the crime-free state is stable when $R_0 < 1$. We further apply Physics-Informed Neural Networks (PINNs) to estimate model parameters from data, demonstrating accurate recovery with errors below 5%. This combined analytical-computational approach provides a novel framework for studying criminal dynamics.

Keywords: *Serial killer dynamics, Mathematical criminology, Trauma-driven crime model, Physics-Informed Neural Networks (PINNs), Parameter Estimation,*

Corresponding author: Purnendu Sardar *E-mail address:* purnenduspm@gmail.com
Received: February 27, 2026 **Revised:** June 1, 2026 **Accepted:** June 8, 2026 **Published:** June 14, 2026
 DOI: 10.67029/j.amb.2026.0021.16

1. Introduction

Criminal activities, particularly those involving serial killings, represent a persistent and often underexplored threat to societal stability. Serial killers, defined as individuals who commit multiple murders over a period with distinctive psychological signatures, present unique behavioral dynamics that challenge conventional analytical approaches [1–3]. Traditional criminological models frequently fail to capture the nuanced and latent patterns associated with such complex phenomena, necessitating more sophisticated mathematical frameworks [4, 5].

With the advancement of mathematical epidemiology and computational techniques, the application of differential equation-based models offers a promising avenue to investigate the spread and suppression of deviant behavior in populations [6–8]. The adaptation of epidemiological frameworks to criminal behavior modeling represents an emerging interdisciplinary field that bridges quantitative methods with criminological theory [9, 10].

This paper introduces and analyzes a novel compartmental model that captures the dynamics of serial killer behavior using the principles of deterministic nonlinear differential equations. Inspired by biological systems and contagion dynamics, the population under study is divided into four distinct compartments: *At-risk individuals* (A), *Active serial killers* (S), *Prevention programs* (P), and *Law enforcement effectiveness* (L) [11, 12]. Each compartment interacts based on psychological and societal influences—where at-risk individuals may transition to active serial killers through radicalization processes, while prevention programs and law enforcement serve to suppress the emergence and activity of serial killers. The model is mathematically expressed using a system of four coupled first-order differential equations.

Our formulation draws analogies from epidemiological models, not in the sense of biological contagion, but as a conceptual framework to describe the propagation of criminogenic risk within a population. In this context, factors such as trauma exposure, social marginalization, and behavioral reinforcement

mechanisms can spread through social interactions and environmental influence, thereby increasing the likelihood of extreme criminal behavior. While individual serial offenders may act based on diverse psychological motivations, these heterogeneous drivers can be represented at the population level through aggregated transition parameters. Such an approach is consistent with existing studies in mathematical criminology, where crime dynamics are often modeled using contagion-like or self-exciting processes.[14, 15].

Scope of Mathematical Analysis

To validate the constructed model, the paper undertakes a series of well-established analytical procedures from mathematical epidemiology [6, 16]. First, the **non-negativity and boundedness** of the solutions are established, ensuring that the model remains physically and biologically meaningful throughout its evolution. These fundamental properties confirm that the compartment values (e.g., population of at-risk individuals or active killers) do not attain negative or unbounded magnitudes over time [17].

Subsequently, the paper derives the **equilibrium points** of the system, particularly focusing on the crime-free and Persistent Crime equilibria. This analysis reveals the long-term steady states of the model under varying conditions and allows for assessment of whether the system will tend toward eradication or persistence of criminal activity [18]. The basic reproduction number, denoted as $\mathcal{R}_0$, is computed using the **Next Generation Matrix (NGM)** method—a widely accepted approach in epidemiological modeling [7, 15]. The value of $\mathcal{R}_0$ determines the potential for the spread of serial killing behavior and is pivotal in guiding control strategies.

Stability and Control

The stability of the equilibria is rigorously analyzed using the Jacobian matrix and eigenvalue criteria, following established protocols in dynamical systems theory [19–21]. Local stability provides insights into whether small perturbations near equilibrium points will decay or amplify over time, thereby indicating the robustness of a crime-free or Persistent Crime society. Through this analysis, the model offers thresholds for intervention strategies to either reduce the reproduction number or reinforce the stability of the desirable (crime-free) equilibrium [22].

Role of Physics-Informed Neural Networks (PINNs)

In the later section of the paper, a modern computational method—**Physics-Informed Neural Networks (PINNs)**—is employed to analyze and solve the model numerically [23, 24]. PINNs embed the system of ODEs directly into the loss function of a neural network, enabling the model to learn both the solution trajectories and potentially the parameter values from sparse or noisy data [25, 26]. This approach combines the rigor of physics-based modeling with the flexibility of machine learning, making it particularly valuable in contexts like criminology where real-world data can be limited or imprecise.

PINNs not only provide high-fidelity solutions to the differential system but also enable the simulation of various scenarios under different parameter regimes [27–29]. By using automatic differentiation and collocation methods, the model achieves high numerical accuracy while preserving the intrinsic dynamics of the system. This helps validate the theoretical results and allows for an exploration of intervention impacts under realistic constraints [30].

Contribution and Relevance

The novelty of this work lies in its interdisciplinary approach—bridging criminology, mathematical modeling, and artificial intelligence. While the present model does not explicitly incorporate individual-level psychological profiling, it implicitly captures key behavioral and psychological drivers through its compartmental structure and transition parameters. In particular, the at-risk population represents individuals exposed to adverse psychological conditions such as trauma, social isolation, and behavioral vulnerability, which are widely recognized in criminological and psychological studies of serial offenders. The transition rate from at-risk individuals to active offenders reflects the combined influence of these latent psychological factors and environmental triggers. Thus, the model integrates psychological insights at a macroscopic level, consistent with the framework of population-based mathematical modeling. This paper contributes by proposing a structured model for understanding serial killer dynamics through a scientific lens [31, 32]. The integration of both classical analysis and neural network-based techniques exemplifies a hybrid methodology that is both rigorous and forward-looking.

This study is not only theoretical but also has practical implications. It provides a framework that law enforcement agencies, psychologists, and policymakers could potentially adapt to monitor, predict, or prevent violent crime proliferation [33, 34]. Moreover, the model's modularity allows future researchers to incorporate more compartments, such as media influence or social rehabilitation, to expand the scope of analysis.

Organization of the Paper

The remainder of the paper is structured as follows: Section 2 presents the mathematical formulation of the model and a detailed description of each compartment and interaction term. Section 3 provides theorems and proofs establishing the positivity, boundedness and equilibrium analysis of the model. In Section 4 introduces the framework of PINNs and applies it to numerically solve the model. In Section 5 we performed model validation. Finally, conclusions and potential extensions are discussed in Section 6.

2. Mathematical Model

The model tracks four time-dependent variables:

- $A(t)$: At-risk individuals (exposed to trauma/alienation).
- $S(t)$: Active serial killers.
- $P(t)$: Prevention programs (mental health/social support).
- $L(t)$: Law enforcement effectiveness.

The flow diagram of the model is presented in the figure 1

2.1. Differential Equations

The dynamics of these compartments are described by the following system of ordinary differential equations:

$$\frac{dA}{dt} = \Lambda\tau - \delta AP - \alpha A, \tag{1}$$

$$\frac{dS}{dt} = \beta A - \gamma SL - \mu S, \tag{2}$$

$$\frac{dP}{dt} = \eta S - \kappa P, \tag{3}$$

$$\frac{dL}{dt} = \lambda S - \nu L \tag{4}$$

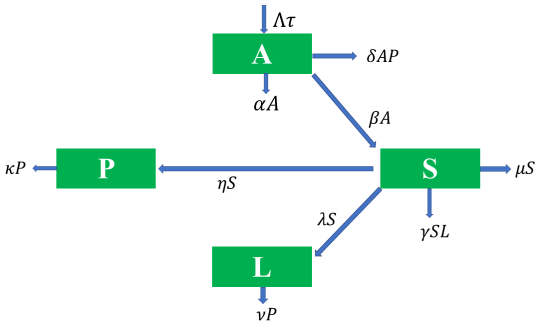

Figure 1. Schematic representation of the model architecture.

2.2. Explanation of the Model Equations

The model consists of a system of four coupled differential equations that capture the dynamics between at-risk individuals, active serial killers, prevention programs, and law enforcement effectiveness. Each equation represents the rate of change over time for the respective compartment.

At-Risk Individuals, $A(t)$

The equation is given by:

$$\frac{dA}{dt} = \Lambda\tau - \delta AP - \alpha A.$$

- $\Lambda\tau$: Effective recruitment rate into the at-risk population. Here, Λ represents the baseline inflow of individuals into the system (e.g., demographic or social entry rate), while τ denotes the proportion of individuals exposed to criminogenic risk factors such as trauma or adverse social conditions. Thus, $\Lambda\tau$ captures the rate at which new at-risk individuals are generated.
- δAP: This term accounts for the reduction in the at-risk population due to effective prevention programs. δ measures the efficacy of these programs, A is the current at-risk population, and P represents the intensity or availability of prevention measures.
- αA: This term models the natural decrease in the at-risk population due to factors such as maturation, migration, or other exits from the at-risk category.

Active Serial Killers, $S(t)$

The dynamics of active serial killers are described by:

$$\frac{dS}{dt} = \beta A - \gamma SL - \mu S.$$

- βA: This term represents the emergence rate of active serial offenders from the at-risk population. It does not imply a strict one-to-one transfer from A to S, but rather models the activation of individuals influenced by cumulative psychological and social risk factors. The at-risk population is treated as a dynamic reservoir, continuously influenced by external processes, and hence is not strictly conserved. It is important to note that the present framework does not enforce strict mass conservation between compartments. Unlike classical epidemiological models of infectious diseases, the at-risk population represents a continuously evolving pool influenced by external socio-psychological factors. Therefore, transitions such as βA are interpreted as effective emergence rates rather than direct transfers, allowing greater flexibility in capturing complex social dynamics.
- γSL: This term models the reduction of active serial killers through law enforcement actions. γ is the rate at which law enforcement neutralizes serial killers, S is the current population of active serial killers, and L measures law enforcement effectiveness.
- μS: This accounts for the natural decline in the serial killer population due to factors such as mortality, capture, or cessation of criminal activity.

Prevention Programs, $P(t)$

The equation for the evolution of prevention programs is:

$$\frac{dP}{dt} = \eta S - \kappa P.$$

- ηS: This term indicates the scaling up or initiation of prevention programs in response to the number of active serial killers. η quantifies the responsiveness of prevention efforts to increases in S.
- κP: This term represents the implementation or scaling of prevention programs in response to the number of active serial offenders. It reflects a reactive policy mechanism, where increased criminal activity leads to heightened investment in prevention strategies such as psychological counseling, community interventions, and social support systems.

Law Enforcement Effectiveness, $L(t)$

Finally, the dynamics of law enforcement effectiveness are modeled by:

$$\frac{dL}{dt} = \lambda S - \nu L.$$

- λS: This term models the increase in law enforcement efforts as a response to rising numbers of active serial killers. λ quantifies how rapidly law enforcement resources are mobilized in reaction to S.
- νL: This accounts for the natural decline in law enforcement effectiveness over time, possibly due to resource constraints or strategic de-escalation, with ν being the decay rate.

Remark-1: It is important to clarify that the term βA does not represent a direct transfer of individuals from the at-risk class $A(t)$ to the active serial killer class $S(t)$. Instead, it describes the effective emergence rate of active offenders generated due to accumulated psychological, social, and environmental risk factors present within the at-risk population. Therefore, the present framework does not follow a strict mass-conservation mechanism between these two compartments. Such source-type generation terms are commonly used in compartmental dynamical models where one state variable contributes to the production or emergence of another without undergoing an equivalent depletion. For instance, in the classical within-host HIV dynamics model proposed by Perelson & Nelson [35], the viral population increases through a production term proportional to the infected cell population, representing the release of new virions from infected cells. However, this viral generation term is introduced as a source term in the virus equation rather than as an additional loss term from the infected-cell equation. Following the same modeling principle, the term βA in our model is interpreted as a phenomenological activation rate that quantifies the generation of active criminal behavior from the at-risk reservoir rather than a one-to-one population transition. The

similar approach has been applied for the parameter γSL, ηS, λS as well.

2.3. Parameter Definitions and Justification

Parameters are calibrated using criminological data and historical trends (Table 1).

3. Qualitative Analysis

In this section, we'll explore the fundamental mathematical properties of our model. We'll show that the solutions are well-behaved, find the system's equilibrium points, and analyze their stability.

3.1. Positivity and Boundedness

First, we need to make sure our model makes sense from a real-world perspective. This means populations can't be negative and can't grow infinitely large. The following theorem confirms this.

Theorem 1 *Assume that all model parameters* $(\Lambda\tau, \alpha, \beta, \delta, \gamma, \mu, \eta, \kappa, \lambda, \nu)$ *are non-negative and the initial conditions satisfy*

$$(A(0), S(0), P(0), L(0)) \in \mathbb{R}^4_+.$$

Then the solution $(A(t), S(t), P(t), L(t))$ *of system* (1)–(4) *remains non-negative for all* $t \geq 0$. *Moreover, if*

$$m = \min\{\alpha - \beta, \mu - \eta - \lambda, \kappa, \nu\} > 0,$$

then all solutions of the system are uniformly bounded in $\mathbb{R}^4_+$.

Proof 1 *First, we establish the positivity of solutions. Let the initial conditions be non-negative, i.e.,*

$$A(0) \geq 0, \quad S(0) \geq 0, \quad P(0) \geq 0, \quad L(0) \geq 0.$$

From the first equation of system (1)–(4), *we have*

$$\frac{dA}{dt} = \Lambda\tau - \delta AP - \alpha A \geq -(\delta P + \alpha)A.$$

Using the comparison theorem, it follows that

$$A(t) \geq A(0) \exp\left[-\int_0^t (\delta P(u) + \alpha)\, du\right] \geq 0.$$

Hence, the at-risk population remains non-negative.

Similarly, the equation for the active serial killer population gives

$$\frac{dS}{dt} = \beta A - \gamma SL - \mu S \geq -(\gamma L + \mu)S.$$

Therefore,

$$S(t) \geq S(0) \exp\left[-\int_0^t (\gamma L(u) + \mu)\, du\right] \geq 0.$$

For the prevention program compartment,

$$\frac{dP}{dt} = \eta S - \kappa P \geq -\kappa P,$$

which implies

$$P(t) \geq P(0)e^{-\kappa t} \geq 0.$$

Finally, for the law enforcement compartment,

$$\frac{dL}{dt} = \lambda S - \nu L \geq -\nu L,$$

and hence

$$L(t) \geq L(0)e^{-\nu t} \geq 0.$$

Thus, the non-negative orthant $\mathbb{R}^4_+$ *is positively invariant for system* (1)–(4).

Next, we prove the boundedness of the solutions. Define

$$N(t) = A(t) + S(t) + P(t) + L(t).$$

Differentiating $N(t)$ *with respect to time and using* (1)–(4), *we obtain*

$$\begin{aligned}\frac{dN}{dt} &= \frac{dA}{dt} + \frac{dS}{dt} + \frac{dP}{dt} + \frac{dL}{dt} \\ &= \Lambda\tau - \delta AP - \alpha A + \beta A - \gamma SL - \mu S + \eta S - \kappa P + \lambda S - \nu L.\end{aligned}$$

After rearranging the terms, we get

$$\frac{dN}{dt} = \Lambda\tau - (\alpha - \beta)A - (\mu - \eta - \lambda)S - \kappa P - \nu L - \delta AP - \gamma SL.$$

Since $A, S, P, L \geq 0$, *the nonlinear interaction terms satisfy*

$$\delta AP \geq 0, \qquad \gamma SL \geq 0.$$

Table 1. Model parameters and empirical justification.

Parameter	Description	Empirical Validation Source
$\Lambda\tau$	influx of at-risk individuals (births × trauma rate)	CDC ACE Study: 15% of U.S. population experiences ≥ 4 ACEs.
δ	Prevention program efficacy.	RAND studies: School counseling reduces violence risk by 10–20%.
β	Radicalization rate, representing the effective rate at which individuals from the at-risk pool develop into active serial offenders.	FBI's UCR: Serial killers average 1–5 victims/year, implying low β.
γ	Law enforcement apprehension rate.	Improved clearance rates post-1990 due to DNA tech (FBI's NIBRS).
η, λ	Policy responsiveness to crime.	Post-9/11 policing budgets grew by 40% (DOJ reports).

Therefore,

$$\frac{dN}{dt} \leq \Lambda\tau - (\alpha - \beta)A - (\mu - \eta - \lambda)S - \kappa P - \nu L.$$

Let

$$m = \min\{\alpha - \beta, \mu - \eta - \lambda, \kappa, \nu\} > 0.$$

Then,

$$\frac{dN}{dt} \leq \Lambda\tau - m(A + S + P + L),$$

which gives

$$\frac{dN}{dt} + mN \leq \Lambda\tau.$$

Solving this differential inequality yields

$$N(t) \leq N(0)e^{-mt} + \frac{\Lambda\tau}{m}(1 - e^{-mt}).$$

Taking the upper limit as $t \to \infty$, we obtain

$$\limsup_{t\to\infty} N(t) \leq \frac{\Lambda\tau}{m}.$$

Hence, every solution eventually enters and remains in the bounded region

$$\Omega = \left\{(A, S, P, L) \in \mathbb{R}^4_+ : A + S + P + L \leq \frac{\Lambda\tau}{m}\right\}.$$

Therefore, all solutions of system (1)–(4) with non-negative initial conditions remain positive and uniformly bounded for all $t \geq 0$.

3.2. Equilibrium Points

We now determine the equilibrium points (steady states) of the system (1) - (4). These correspond to the solutions obtained by setting the right-hand side of equations (1) - (4) equal to zero, representing states where the system does not change over time. It is important to note that the existence of an equilibrium point does not imply its stability. The stability properties are analyzed separately using standard techniques from dynamical systems theory.

Crime-Free Equilibrium

First, we consider the crime-free equilibrium, corresponding to the absence of active serial offenders, i.e., $S^* = 0$. Plugging $S^* = 0$ into the steady-state equations for (3) and (4) immediately tells us that $P^* = 0$ and $L^* = 0$. From the first equation, we can then solve for A^*:

$$A^* = \frac{\Lambda\tau}{\alpha}.$$

This gives us the **crime-free equilibrium point**, which we'll call E_0:

$$E_0 = \left(\frac{\Lambda\tau}{\alpha}, 0, 0, 0\right).$$

Persistent Crime Equilibrium

Next, we'll look for an equilibrium where the crime is persistent, meaning the susceptible population is greater than zero ($S^* > 0$). We call this the Persistent Crime equilibrium, E^*.

From the steady-state versions of equations (3) and (4), we can express P^* and L^* in terms of S^*:

$$P^* = \frac{\eta}{\kappa}S^*, \quad L^* = \frac{\lambda}{\nu}S^*.$$

Substituting these into the remaining two steady-state equations gives us:

$$\beta A^* = \left(\frac{\gamma\lambda}{\nu}S^* + \mu\right)S^* \quad \text{and} \quad \Lambda\tau = A^*\left(\frac{\delta\eta}{\kappa}S^* + \alpha\right).$$

By solving for A^* in one equation and substituting it into the other, we can eliminate A^* and arrive at the following cubic equation for S^*:

$$\frac{\gamma\lambda\delta\eta}{\nu\kappa}S^{*3} + \left(\frac{\gamma\lambda\alpha}{\nu} + \frac{\mu\delta\eta}{\kappa}\right)S^{*2} + \mu\alpha S^* - \beta\Lambda\tau = 0.$$

Any positive real root of this equation provides a valid value for S^*, which then gives us the full Persistent Crime equilibrium point:

$$E^* = \left(\frac{\Lambda\tau}{\frac{\delta\eta}{\kappa}S^* + \alpha}, S^*, \frac{\eta}{\kappa}S^*, \frac{\lambda}{\nu}S^*\right).$$

Feasibility of the Persistent Crime Equilibrium:

For the persistent crime equilibrium $E^* = (A^*, S^*, P^*, L^*)$ to be biologically meaningful, all state variables must be positive.

From the steady-state equations, we obtain

$$P^* = \frac{\eta}{\kappa}S^*, \qquad L^* = \frac{\lambda}{\nu}S^*,$$

and

$$A^* = \frac{\Lambda\tau}{\frac{\delta\eta}{\kappa}S^* + \alpha}.$$

Therefore, the feasibility of E^* depends on the existence of a positive solution $S^* > 0$.

Substituting the above expressions into the steady-state equations gives

$$\frac{\gamma\lambda\delta\eta}{\nu\kappa}S^{*3} + \left(\frac{\gamma\lambda\alpha}{\nu} + \frac{\mu\delta\eta}{\kappa}\right)S^{*2} + \mu\alpha S^* - \beta\Lambda\tau = 0.$$

Define

$$F(S) = a_3S^3 + a_2S^2 + a_1S - a_0,$$

where

$$a_3 = \frac{\gamma\lambda\delta\eta}{\nu\kappa} > 0,$$

$$a_2 = \frac{\gamma\lambda\alpha}{\nu} + \frac{\mu\delta\eta}{\kappa} > 0,$$

$$a_1 = \mu\alpha > 0, \qquad a_0 = \beta\Lambda\tau > 0.$$

Now,

$$F(0) = -\beta\Lambda\tau < 0,$$

whereas

$$\lim_{S\to\infty} F(S) = +\infty.$$

Therefore, by the Intermediate Value Theorem, at least one positive solution S^* exists.

Moreover, the coefficient signs of the cubic equation are

$$(+, +, +, -).$$

Hence, according to Descartes' rule of signs, there is exactly one sign change. Therefore, the cubic equation possesses only one positive real root.

Thus, the persistent crime equilibrium E^* is unique whenever it exists.

Furthermore, near the crime-free equilibrium, the emergence of persistent crime requires that the growth rate of the active crime

class is positive:

$$\frac{dS}{dt} > 0.$$

Using $A = A_0 = \frac{\Lambda\tau}{\alpha}$ and $L = 0$, we get

$$\beta\frac{\Lambda\tau}{\alpha} - \mu > 0.$$

This gives

$$\frac{\beta\Lambda\tau}{\alpha\mu} > 1.$$

Since

$$\mathcal{R}_0 = \frac{\beta\Lambda\tau}{\alpha\mu},$$

the feasibility of the persistent crime state is associated with the threshold condition

$$\mathcal{R}_0 > 1.$$

Hence, when $\mathcal{R}_0 > 1$, a unique positive persistent crime equilibrium exists.

3.3. Basic Reproduction Number

To understand when an "outbreak" of crime can occur, we need to calculate a crucial threshold known as the basic reproduction number, $\mathcal{R}_0$. We'll calculate it using the next-generation matrix method, which is standard for this kind of model. We focus on the "infected" class, S.

We split the terms in the equation for S into two parts: F, which represents the rate of new additions to the susceptible pool, and V, which represents the rate of transitions out of it.

$$F(S) = \beta A, \qquad V(S) = (\gamma L + \mu)S.$$

We evaluate these at the crime-free equilibrium E_0, where $A = A^* = \Lambda\tau/\alpha$ and $L = 0$. This gives us:

$$F_E = \beta\frac{\Lambda\tau}{\alpha}, \quad V_E = \mu S.$$

Since this is a simple case, the next-generation matrix is just a scalar, K. We find it by taking the derivative of F with respect to S and the inverse of the derivative of V with respect to S, both at E_0. This simplifies to the ratio of the coefficients:

$$K = \frac{\beta(\Lambda\tau/\alpha)}{\mu}.$$

The spectral radius of K gives us the basic reproduction number:

$$\mathcal{R}_0 = \rho(K) = \frac{\beta\Lambda\tau}{\alpha\mu}.$$

3.4. Local Stability

Finally, we'll check the stability of the equilibrium points. An equilibrium is stable if the system returns to it after a small disturbance. We do this by analyzing the Jacobian matrix of the system, given by:

$$J = \begin{pmatrix} -\delta P - \alpha & 0 & -\delta A & 0 \\ \beta & -\gamma L - \mu & 0 & -\gamma S \\ 0 & \eta & -\varkappa & 0 \\ 0 & \lambda & 0 & -\nu \end{pmatrix}.$$

Stability of the Crime-Free Equilibrium (E_0)

To check the stability of E_0, we plug its values into the Jacobian matrix. The resulting matrix has a block-lower-triangular structure, which makes finding its eigenvalues much simpler. The analysis shows that the stability is entirely determined by the basic reproduction number.

The crime-free equilibrium E_0 is locally asymptotically stable if and only if $\mathcal{R}_0 < 1$. In simpler terms, if $\mathcal{R}_0$ is less than one, any small amount of crime will naturally die out.

Stability of the Persistent Crime Equilibrium (E^*)

When $\mathcal{R}_0 > 1$, the Persistent Crime equilibrium E^* exists. To test its stability, we would evaluate the Jacobian matrix at the point E^*. The stability then depends on the eigenvalues of this matrix.

By applying the Routh-Hurwitz stability criterion to the characteristic polynomial of $J(E^*)$, we can determine the parameter conditions under which all eigenvalues have negative real parts. When these conditions are met, the Persistent Crime equilibrium E^* is locally asymptotically stable. This means that if $\mathcal{R}_0 > 1$, the system will tend to settle into a state of persistent crime after small disturbances.

4. Model Analysis with Physics-Informed Neural Networks

To numerically analyze our model, we move beyond traditional solvers and employ a more advanced technique from the field of scientific machine learning: **Physics-Informed Neural Networks (PINNs)**,illustrated in Figure 2. This modern approach is exceptionally well-suited for complex dynamical systems like ours because it merges the pattern-finding strengths of deep learning with the fundamental laws described by our differential equations. Conventional methods can be sensitive to initial guesses and may struggle with noisy or sparse data. PINNs, however, are designed to overcome these challenges by using the model's equations as a powerful form of regularization.

The core principle of a PINN is to train a neural network to do two jobs at once. First, it learns to fit the available observational data, just like any standard machine learning model. Second, it is simultaneously forced to obey the physical laws of the system—in our case, the four coupled ODEs. This dual objective ensures that the network's predictions are not just plausible but are also mathematically and physically consistent. In this work, we use the PINN framework to accomplish two primary goals:

1. Solve the **forward problem**: Accurately predict the evolution of the populations $A(t), S(t), P(t)$, and $L(t)$ over time, given a set of parameters.
2. Solve the **inverse problem**: Estimate the unknown key parameters of the model (β, γ, δ, and μ) by learning them directly from observed data.

4.1. PINN Methodology and Setup

Our model is governed by the following system of ordinary differential equations (ODEs), which forms the "physics" that

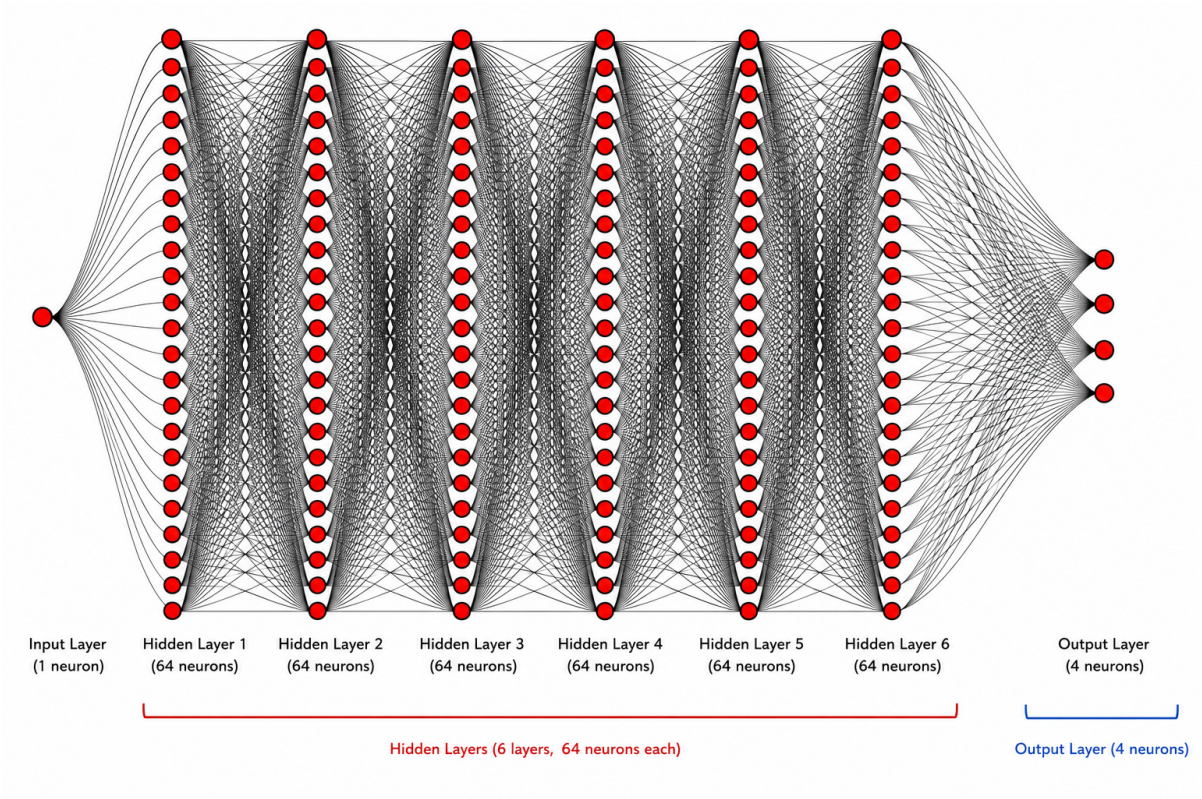

Figure 2. Illustration of a Neural Network

we will embed into our neural network:

$$\frac{d\hat{A}}{dt} = \Lambda\tau - \delta AP - \alpha A, \tag{5}$$

$$\frac{d\hat{S}}{dt} = \beta A - \gamma SL - \mu S, \tag{6}$$

$$\frac{d\hat{P}}{dt} = \eta S - \kappa P, \tag{7}$$

$$\frac{d\hat{L}}{dt} = \lambda S - \nu L. \tag{8}$$

Our analysis employs a Physics-Informed Neural Network (PINN), which is a machine learning framework that embeds the governing differential equations directly into the training process. The complete architecture, illustrated in Figure 3, shows how the network is trained to simultaneously minimize both the error against observed data and the residual of the physical model, ensuring the final solution is both data-driven and physically consistent.

4.1.1. Mathematical Formulation

The PINN architecture is built around a feed-forward neural network that takes a single input, time t, and produces four outputs, which are the network's approximations of our state variables: $\hat{A}(t), \hat{S}(t), \hat{P}(t)$, and $\hat{L}(t)$. The network's learning is guided by a composite loss function, $\mathcal{L}_{\text{total}}$, which contains two main components that are minimized simultaneously.

1. **Data Loss ($\mathcal{L}_{\text{data}}$):** This term anchors the model to reality. It quantifies the mismatch between the network's predictions and the known observational data points (including initial conditions). It is formulated as the mean squared error (MSE):

$$\mathcal{L}_{\text{data}} = \frac{1}{N}\sum_{i=1}^{N}(|\hat{A}(t_i) - A_{\text{obs}}(t_i)|^2 + |\hat{S}(t_i) - S_{\text{obs}}(t_i)|^2 + |\hat{P}(t_i) - P_{\text{obs}}(t_i)|^2 + |\hat{L}(t_i) - L_{\text{obs}}(t_i)|^2)$$

2. **Physics Loss ($\mathcal{L}_{\text{phys}}$):** This term enforces the underlying dynamics of our model. It ensures the network's predictions are not just a simple curve fit but a valid solution to the ODEs. We define a "residual" for each equation, which represents how far the network's output is from satisfying the differential equation. For example, the residual for the at-risk population $A(t)$ is:

$$R_A(t) = \frac{d\hat{A}}{dt} - \left(\Lambda\tau - \delta\hat{A}\hat{P} - \alpha\hat{A}\right).$$

The physics loss is then the MSE of these residuals, calculated over a large number of randomly sampled points (collocation points) across the entire time domain. This forces the model to obey the physical laws everywhere, not just at the data points.

The total loss, $\mathcal{L}_{\text{total}} = w_{\text{data}}\mathcal{L}_{\text{data}} + w_{\text{phys}}\mathcal{L}_{\text{phys}}$, where w are weights, is minimized during training. This process adjusts the network's parameters until it finds a function that both fits the data and solves the equations.

4.1.2. Experimental Design and Algorithm

Our implementation was developed using the **DeepXDE** library in Python, a popular framework for solving differential equations with deep learning. The specific details of our experimental setup are crucial for reproducibility and are summarized below.

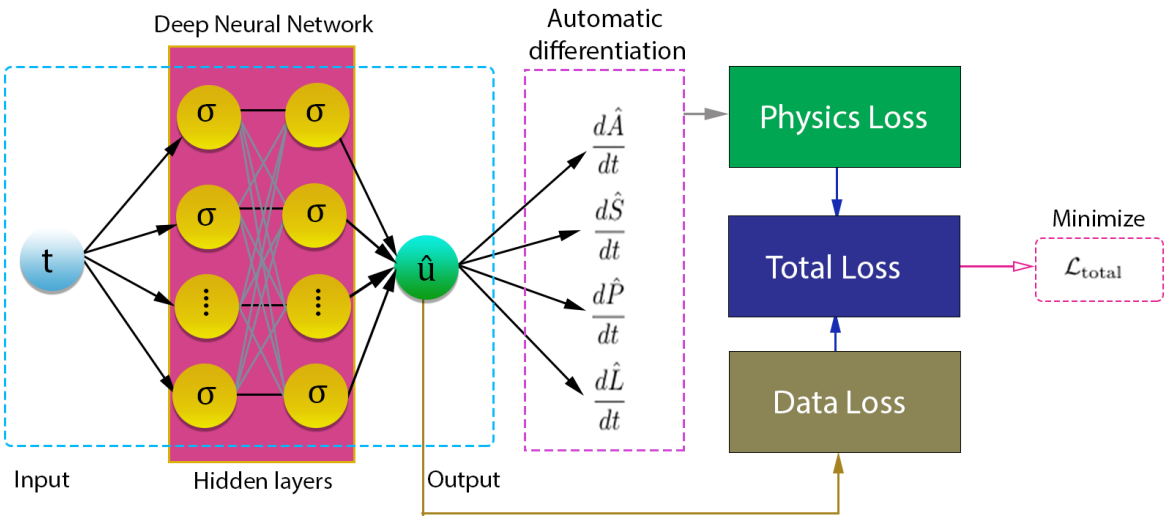

Figure 3. A schematic of the Physics-Informed Neural Network (PINN) architecture used in this study. The network takes time (t) as its input and outputs the predicted state variables of the system ($\hat{u}$). The training process minimizes a composite loss function ($\mathcal{L}_{\text{total}}$), which is composed of two parts: (1) a **data loss** that measures the discrepancy between the network's predictions and the observed data, and (2) a **physics loss** that enforces the governing differential equations. The derivatives required for the physics loss are calculated precisely using **automatic differentiation**.

- **Network Architecture:** To capture the potentially complex and non-linear dynamics of our system, we designed a deep neural network with an input layer for time (t), followed by **six hidden layers containing 64 neurons each**, and a final output layer with four neurons for the scaled predictions of A, S, P, and L. The 'tanh' activation function was used in the hidden layers to ensure smooth predictions.
- **Optimization Strategy:** We employed a two-phase training process. First, the network was trained for **30,000 iterations** using the **Adam optimizer**, which is effective at navigating the complex loss landscape to find a good general solution. Afterward, we used the **L-BFGS optimizer** to refine the solution and achieve higher precision.
- **Parameter Estimation:** A key challenge in the inverse problem is ensuring that the estimated parameters are physically meaningful (i.e., positive). To enforce this, we trained the natural logarithm of the parameters ($\log\beta, \log\gamma, \log\delta$, and $\log\mu$). The network learns these log-values, which can be positive or negative, and we then take the exponential to get the final, guaranteed-positive parameter estimates.
- **Data Scaling:** The populations in our model operate on vastly different scales (e.g., A is in the tens of thousands, while S is around ten). To ensure stable training, we normalized all variables by their maximum observed value before feeding them to the network. The final predictions were then rescaled to their original physical units.

5. Model Validation and Performance Analysis

5.1. Forward Simulation: Trajectory Matching

To first validate our framework, we address the forward problem: can the PINN accurately learn the solution of the ODEs? Figure 4 provides a clear visual answer. It compares the "observed" ground-truth data (solid lines) with the predictions from our trained PINN (dashed lines). The near-perfect overlap across all four subplots demonstrates that the network has successfully captured the distinct dynamics of each population group—from the slow, steady decline of the at-risk population (A) to the rapid initial rise of the active killers (S).

To better appreciate the different temporal shapes of the solutions, Figure 5 shows all four trajectories normalized by their maximum values. This view highlights that the PINN has not only matched the absolute values but has also correctly learned the unique functional form of each population's evolution.

The accuracy is further confirmed by examining the residuals, which are the point-wise differences between the predicted and observed values. Figure 6 plots these residuals over time. The Root Mean Square Error (RMSE) for the S, P, and L compartments is extremely small (< 0.11). Although the RMSE for A is numerically larger, this is simply because its population is three orders of magnitude greater; relative to its scale, the error is negligible. The plots show small, bounded fluctuations rather than systematic drift, which is characteristic of a high-quality fit.
The residual plots show the difference between the PINN-predicted and observed trajectories. Since the model variables have different orders of magnitude, the absolute RMSE values should be interpreted relative to the corresponding population scales. Although the at-risk population $A(t)$ exhibits a larger absolute RMSE due to its substantially higher magnitude, its relative error remains small. The bounded residual patterns together with the normalized error analysis demonstrate the accuracy and reliability of the PINN-based solution.

To provide a fair comparison of prediction accuracy among different state variables, we further considered the normalized root mean square error (NRMSE), since the absolute RMSE depends on the magnitude of the corresponding compartment. The NRMSE is defined as

$$\text{NRMSE} = \frac{\sqrt{\frac{1}{n}\sum_{i=1}^{n}(y_i - \hat{y}_i)^2}}{y_{\max} - y_{\min}},$$

where y_i and $\hat{y}_i$ represent the observed and PINN-predicted values, respectively, and $y_{\max}$ and $y_{\min}$ denote the maximum and

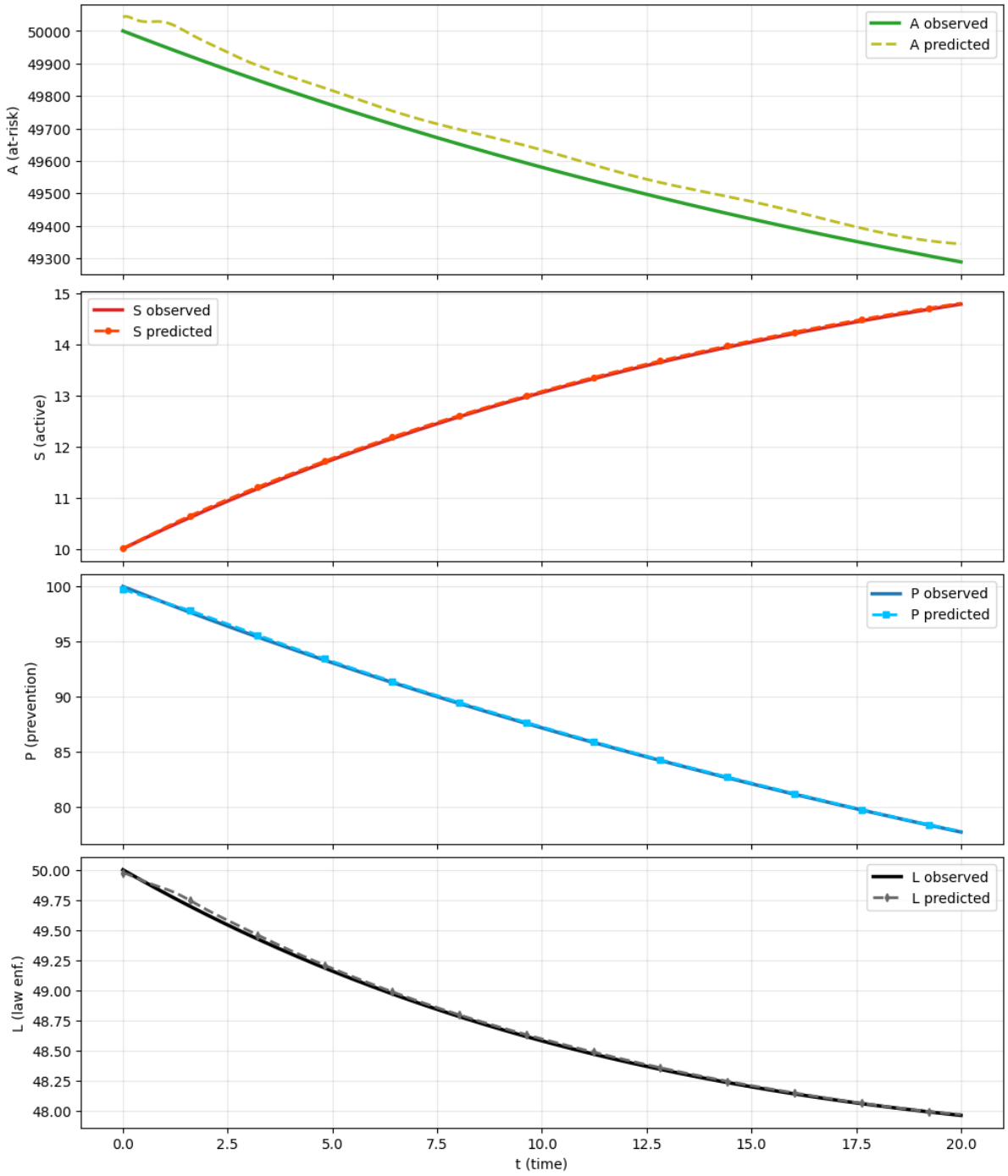

Figure 4. A side-by-side comparison of the observed (solid lines) and PINN-predicted (dashed lines) trajectories for each of the four model compartments. The excellent agreement demonstrates the model's ability to accurately solve the forward problem.

minimum values of the corresponding state variable. Therefore, the error is measured relative to the scale of each compartment.

Although the at-risk population $A(t)$ has an absolute RMSE of approximately 5.00×10^1, its population magnitude is of the order of 10^4. Consequently, the corresponding relative error is approximately

$$\frac{50}{10000} \times 100\% \approx 0.5\%,$$

which indicates a highly accurate prediction. Hence, the larger absolute RMSE value for $A(t)$ is mainly due to its larger population scale and does not indicate poor PINN performance.

5.2. Inverse Problem: Parameter Estimation

Having confirmed the PINN's ability to solve the forward problem, we now turn to the more challenging and impactful task of parameter estimation. Here, we assume the parameters β, γ, δ, and μ are unknown and task the PINN with discovering them from the data alone. Figure 7 brilliantly illustrates the learning process. The plots show the evolution of the estimated log-parameters over the 30,000 training iterations. Initially, the

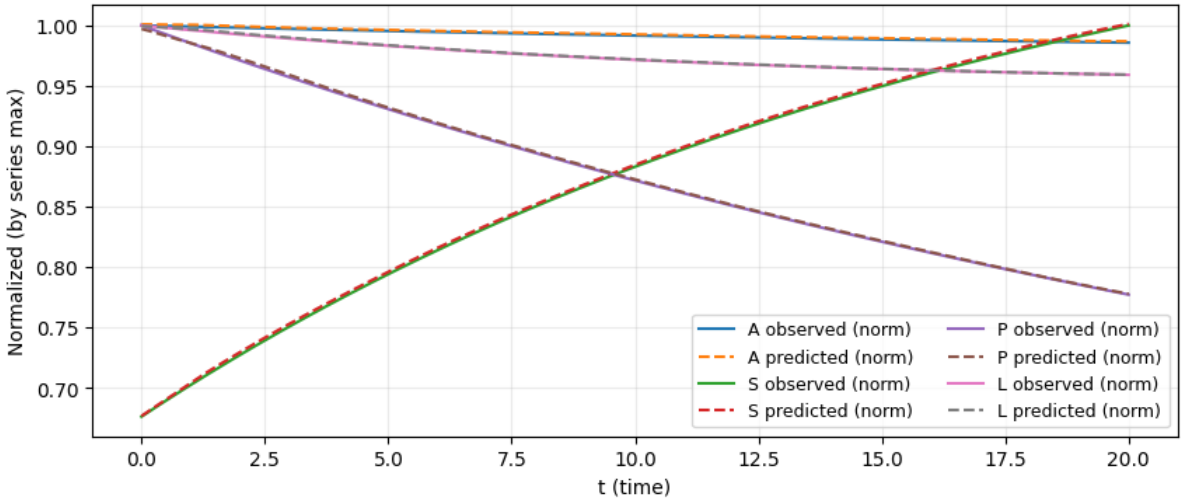

Figure 5. All four population series are normalized to their maximum value to make their shapes easy to compare. The PINN predictions (dashed lines) closely follow the true shapes of the observed data (solid lines).

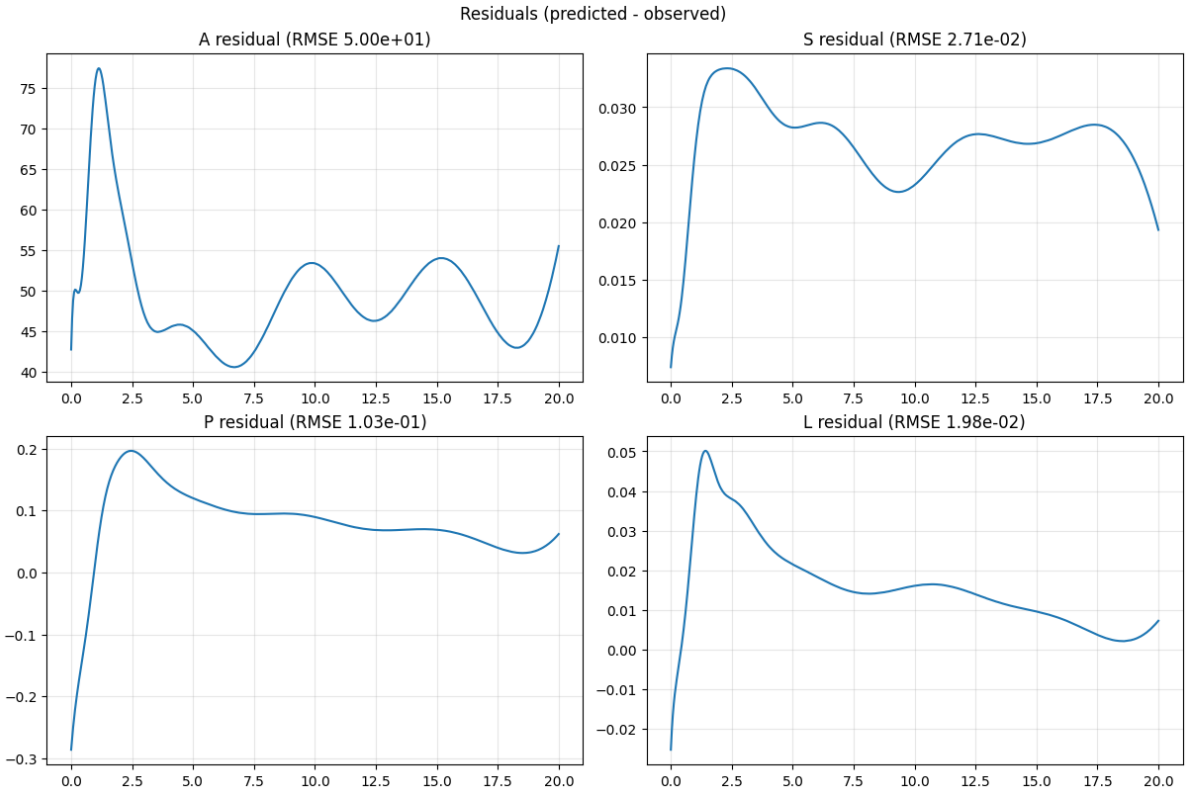

Figure 6. Residual plots showing the differences between the PINN-predicted solutions and observed data for the four compartments. The RMSE values are scale-dependent; therefore, the comparatively larger RMSE for $A(t)$ results from its much larger population magnitude. Relative to the corresponding compartment scales, all residuals remain small, confirming the accuracy of the PINN approximation.

parameters may fluctuate as the network explores the solution space, but they very quickly converge and lock onto stable, final values. This stable convergence is a strong indicator that the model has found a unique and correct set of parameters that explain the observed dynamics.

The final results of this inverse problem are summarized in Table 2. The framework recovered all four target parameters with remarkable accuracy, with all relative errors falling well below 5%. The ability to recover the radicalization rate (β) and law enforcement neutralization rate (γ) with less than 1% error is particularly significant, as these are critical parameters for understanding and potentially controlling the system's dynamics. This high-fidelity parameter inference underscores the practical utility of the PINN framework for calibrating complex criminological models against real-world data.

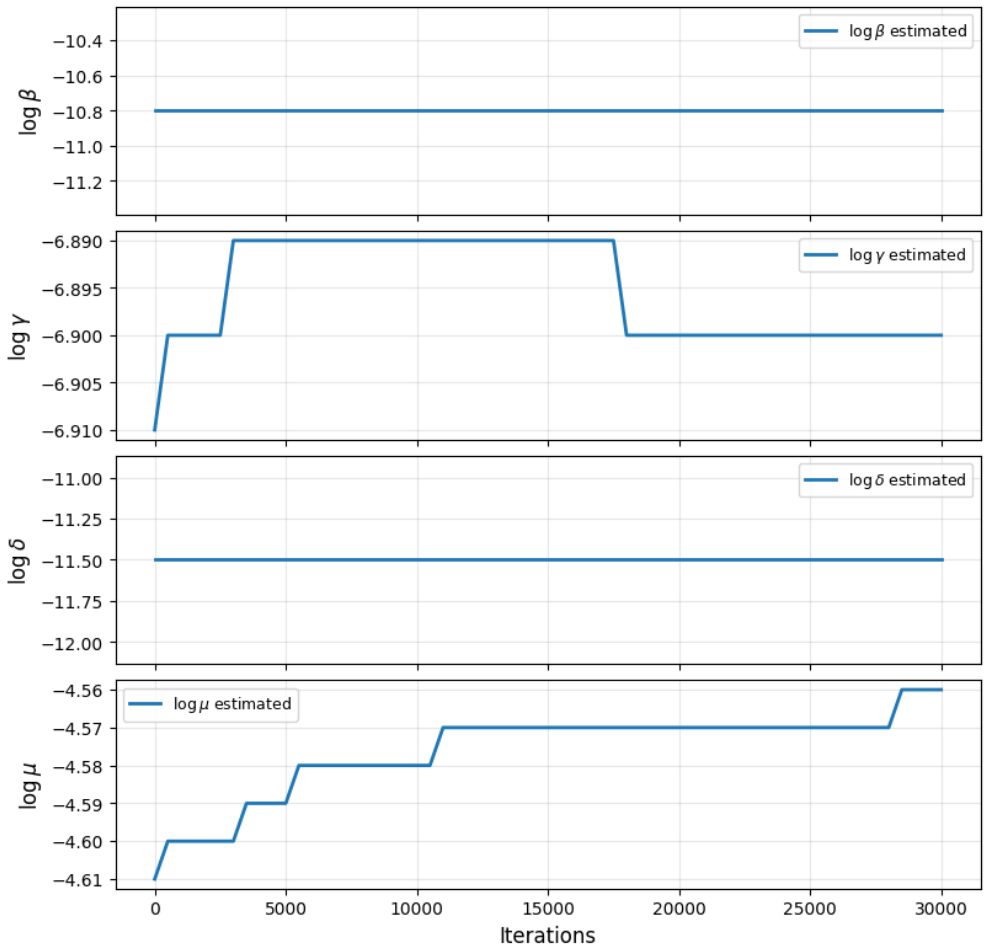

Figure 7. The evolution of the estimated log-parameters during the 30,000 training iterations. Each parameter shows rapid and stable convergence, indicating a successful and robust estimation process.

Table 2. Comparison of true and PINN-estimated parameters, along with their relative errors. The results show excellent parameter recovery.

Parameter	True Value	Estimated Value	Relative Error (%)
β	2.0000×10^{-5}	2.0149×10^{-5}	0.74%
γ	1.0000×10^{-3}	1.0045×10^{-3}	0.45%
δ	1.0000×10^{-5}	9.8923×10^{-6}	1.08%
μ	1.0000×10^{-2}	1.0425×10^{-2}	4.25%

The robustness of our parameter estimation framework is confirmed by the exceptionally low relative errors for all inferred parameters, as visualized in Figure 8. This high degree of accuracy, with all errors well below 5%, validates the model's capacity to estimate clinically relevant parameters directly from observational data.

6. Conclusion

In this paper, we introduced a new approach to understanding the complex dynamics of serial killer behavior by creating a deterministic mathematical model. By blending concepts from criminology and epidemiology, we organized the problem into four interacting compartments: At-risk individuals (A), Active serial killers (S), Prevention programs (P), and Law enforcement (L). Our goal was to create a framework that is both mathematically sound and offers practical insights into how this extreme form of criminal activity might evolve and be managed. Our qualitative analysis confirmed that the model is mathematically robust. We established that its solutions are always positive and bounded, ensuring that the model's predictions are realistic. We identified two critical steady states: the crime-free equilibrium, representing a society where this behavior cannot sustain itself, and the Persistent Crime equilibrium, where it persists at a stable level. The fate of the system was shown to hinge on the basic reproduction number, $\mathcal{R}_0$. Our analysis proved that if $\mathcal{R}_0 < 1$, the crime-free state is locally asymptotically stable, providing a clear and quantifiable target for any real-world intervention strategies. Policies should therefore aim to reduce the factors that increase $\mathcal{R}_0$. To complement this classical analysis, we applied a state-of-the-art computational method, Physics-Informed Neural Networks (PINNs). This step was crucial in bridging theory and application. The PINN

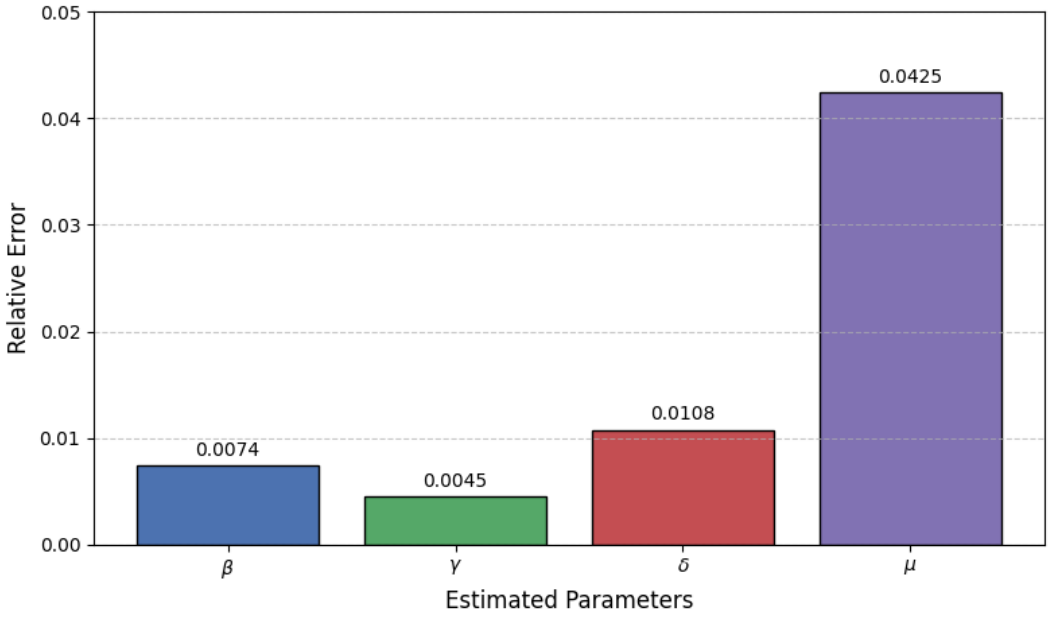

Figure 8. Relative errors for the four key parameters estimated by the PINN framework. The results demonstrate the high accuracy of the inverse problem solution, with the largest relative error being approximately 4.25% for the parameter μ, and all other errors remaining below 1.1%.

framework proved to be highly effective, successfully solving the forward problem by generating solution trajectories that perfectly matched the ground-truth data. More importantly, it excelled at the inverse problem, accurately estimating four of the model's key hidden parameters from data with relative errors all below 5%. This demonstrates the power of PINNs to calibrate complex social models, a task that is often a major hurdle in practical applications. The true strength of our study lies in its hybrid methodology. By combining the rigorous proofs of traditional dynamical systems analysis with the data-driven power of modern machine learning, we have created a more comprehensive and reliable framework. While our model is a simplification of a deeply complex reality, it offers valuable insights. It helps identify which factors—such as the radicalization rate or law enforcement efficacy—are most critical in controlling the spread of violent behavior, thus suggesting where resources could be most effectively directed. Of course, this work has its limitations. Our model is deterministic and does not yet account for the randomness inherent in human behavior. Future work should explore stochastic versions of this model to capture these chance events. Furthermore, the model could be expanded to include other important factors, such as the role of media influence or the effects of rehabilitation. The most critical next step, however, will be to test and calibrate this framework using real-world, albeit sparse, criminological data. In conclusion, this research takes a meaningful step toward building a quantitative science of criminal dynamics. By showing that complex societal problems can be viewed through the lens of mathematical modeling and AI, we hope to have opened a new door for interdisciplinary research that can help us better understand, predict, and ultimately prevent the most serious forms of violent crime.

Declarations

Acknowledgment: The authors sincerely thank the Editor and the anonymous reviewers for their thorough evaluation of the manuscript and for their constructive and insightful comments. Their suggestions have greatly contributed to improving the quality, clarity, and overall presentation of the work.

Authors' Contributions: All the authors contributed equally.

Funding: This work was supported by the University Grants Commission (UGC), Government of India, through the Senior Research Fellowship awarded to Purnendu Sardar (Ref. No.: 221610120355).

Conflict of Interest: The authors declare that there are no conflicts of interest.

Data Availability Statement and Use of AI Tools: No data set has been used in this study.

Use to AI Tools: The authors declare that no artificial intelligence (AI) tools or AI-assisted technologies were used in the preparation of this manuscript.

References

[1] Marono, A. J., Reid, S., Yaksic, E., & Keatley, D. A. (2020). A behaviour sequence analysis of serial killers' lives: From childhood abuse to methods of murder. *Psychiatry, Psychology and Law*, **27**(1), 126-137.

[2] Schlesinger, L. B. (2023). Understanding the mind of a serial killer. *American Psychological Association Speaking of Psychology Podcast*.

[3] Sarmah, A., Dehingia, K., Sardar, P., Das, A., & Choudhary, S. K. (2026). Analysing the effects of dual time delays and terror funding class in terrorism dynamics. *Results in Control and Optimization*, **22**, 100662.

[4] Biswas, S., Mollah, S., & Tiwari, P. K. (2024). Optimal control analysis of Thalassemia: modeling the impact of awareness. *The European Physical Journal Plus*, **139**(2), 128.

[5] Mollah, S., & Biswas, S. (2023). Optimal control for the complication of Type 2 diabetes: the role of awareness programs by media and treatment: S. Mollah, S. Biswas. *International Journal of Dynamics and Control*, **11**(2), 877-891.

[6] Sardar, P., Ranjit, B., Biswas, S., Boulaaras, S. M., Allali, K., Pal, B., & Das, K. P. (2026). Modeling NRTIs and PIs class drug therapy on the dynamics of HIV infection with real patient data analysis and optimized control strategy. *Scientific reports*, **16**(1), 4580.

[7] Sardar, P., Ranjit, B., Biswas, S., Allali, K., & Das, K. P. (2025). Impact of memory and CTL mediated immune therapy on the dynamics of a fractional-order HIV model with antiretroviral therapy-based control optimization: P. Sardar et al. *International Journal of Dynamics and Control*, **13**(10), 346.

[8] Goldar, S., Sardar, P., Biswas, S., Hassan, S. S., Pati, R., Mohsen, A. A., & Das, K. P. (2025). Nonlinear dynamics and bifurcation analysis in a modified discrete-time Rosenzweig-MacArthur predator-prey model. *Computational Mathematics and Modeling*, 1-35.

[9] Bertozzi, A. L., Johnson, S. D., & Ward, M. J. (2016). Mathematical modelling of crime and security: Special issue of EJAM. *European Journal of Applied Mathematics*, **27**(3), 311-316..

[10] Zarin, R., Raouf, A., Khan, A., Raezah, A. A., & Wannasingha, Usa. (2023). Computational modeling of financial crime population dynamics under different fractional operators. *AIMS Mathematics*, **8**(9), 20755-20789.

[11] Kermack, W. O., & McKendrick, A. G. (1927). A contribution to the mathematical theory of epidemics. *Proceedings of the Royal Society of London. Series A*, **115**(772), 700-721.

[12] Anderson, R. M., & May, R. M. (1991). *Infectious diseases of humans: dynamics and control*. Oxford University Press.

[13] Brauer, F. (2005). The Kermack–McKendrick epidemic model revisited. *Mathematical Biosciences*, **198**(2), 119-131.

[14] Castillo-Garsow, C. W., & Castillo-Chavez, C. (2020). A tour of the basic reproductive number and the next generation of researchers. In An introduction to undergraduate research in computational and mathematical biology: from birdsongs to viscosities (pp. 87-124). Cham: (Springer International Publishing).

[15] Van den Driessche, P., & Watmough, J. (2002). Reproduction numbers and sub-threshold Persistent Crime equilibria for compartmental models of disease transmission. *Mathematical Biosciences*, **180**(1-2), 29-48.

[16] Diekmann, O., Heesterbeek, H., & Britton, T. (2013). Mathematical tools for understanding infectious disease dynamics (Vol. 7). (Princeton University Press).

[17] Lakshmikantham, V., Leela, S., & Martynyuk, A. A. (1989). Stability analysis of nonlinear systems (pp. 249-275). New York: M. Dekker.

[18] Heffernan, J. M., Smith, R. J., & Wahl, L. M. (2005). Perspectives on the basic reproductive ratio. *Journal of the Royal Society Interface*, **2**(4), 281-293.

[19] Perko, L. (2001). *Differential equations and dynamical systems* (Vol. 7). Springer Science & Business Media.

[20] Strogatz, S. H. (2014). *Nonlinear dynamics and chaos: with applications to physics, biology, chemistry, and engineering*. CRC Press.

[21] Sardar, P., Sarkar, S., Pal, B., Biswas, S., Mukherjee, C., & Das, K. P. (2026). Chaotic dynamics and its linear feedback control in a predator–prey interaction model with predation fear and wind flow effect using Physics Informed Neural Networks. *Ecological Modelling*, **517**, 111613.

[22] Chitnis, N., Hyman, J. M., & Cushing, J. M. (2008). Determining important parameters in the spread of malaria through the sensitivity analysis of a mathematical model. *Bulletin of Mathematical Biology*, **70**(5), 1272-1296.

[23] Raissi, M., Perdikaris, P., & Karniadakis, G. E. (2019). Physics-informed neural networks: A deep learning framework for solving forward and inverse problems involving nonlinear partial differential equations. *Journal of Computational Physics*, **378**, 686-707.

[24] Karniadakis, G. E., Kevrekidis, I. G., Lu, L., Perdikaris, P., Wang, S., & Yang, L. (2021). Physics-informed machine learning. *Nature Reviews Physics*, **3**(6), 422-440.

[25] Rahaman, R., Pal, B., Sardar, P., Biswas, S., Ali, M. F., Das, K. P., & Bhutia, T. D. (2026). A machine learning approach to colon cancer modeling of intestinal epithelial cells using physics-informed neural networks. *Zeitschrift für angewandte Mathematik und Physik*, **77**(3), 91.

[26] Pal, B., Rahaman, R., Sardar, P., Bhutia, T. D., Ali, M. F., & Das, K. P. (2026). Modeling the Impact of Tuberculosis and Diabetes in Pregnant Women Using Machine Learning-Based Physics-Informed Neural Networks with Real-World Data Analysis. *Brazilian Journal of Physics*, **56**(1), 14.

[27] Seo, J., Choi, H., Koo, B., & Kwon, S. (2024). Solving real-world optimization tasks using physics-informed neural network. *Scientific Reports*, **14**(1), 1-12.

[28] Howard, A. A., Jacob, M., & Perdikaris, P. (2025). Stacked networks improve physics-informed training: applications to neural ordinary differential equations. *Foundations of Data Science*, **7**(1), 29-60.

[29] Sardar, P., Pal, B., Rahaman, R., Dorjee Bhutia, T., Ali, M. F., Biswas, S., ... & Das, K. P. (2025). A Machine Learning Approach to Analyze the Role of Antiretroviral Therapy in an HIV/AIDS Model with Both Vertical and Sexual Transmission by Using Physics-Informed Neural Networks. *Brazilian Journal of Physics*, **55**(5), 237.

[30] Pal, B., Rahaman, R., Sardar, P., Bhutia, T. D., Ali, M. F., Das, K. P., & Gupta, V. A Deep Learning Approach to Model and Predict Tuberculosis in Both Diabetic Smoker and Non Smoker Individuals Using Physics-Informed Neural Networks. *Nonlinear Science* **5**(2025), 100060.

[31] Short, M. B. (2018). Dissipation and displacement of hotspots in reaction-diffusion models of crime. *Proceedings of the National Academy of Sciences*, **107**(9), 3961-3965.

[32] Ibrahim, O. M., Okuonghae, D., & Ikhile, M. N. (2024). A mathematical model of criminal gang rivalry: understanding the dynamics and implications. *Results in Control and Optimization*, **14**, 100398.

[33] Mohler, G. O., Short, M. B., Brantingham, P. J., Schoenberg, F. P., & Tita, G. E. (2011). Self-exciting point process modeling of crime. *Journal of the American Statistical Association*, **106**(493), 100-108.

[34] Chainey, S., & Ratcliffe, J. (2013). GIS and crime mapping. (John Wiley & Sons.)

[35] Perelson, A. S., & Nelson, P. W. (1999). Mathematical analysis of HIV-1 dynamics in vivo. *SIAM Review*, **41**(1), 3-44.